Monomer Cast Polyamide 6 Composites and Their Treatment with High-Energy Electrons

G. Engelmann,[1] U. Gohs,[2] J. Ganster[1]

[1]*Fraunhofer—Institute of Applied Polymer Research, Geiselbergstraße 69, 14476 Potsdam-Golm, Germany*
[2]*Leibniz Institute of Polymer Research Dresden, Hohe Str. 6, D-01069 Dresden, Germany*

Received 16 February 2011; accepted 30 March 2011
DOI 10.1002/app.34593
Published online 12 August 2011 in Wiley Online Library (wileyonlinelibrary.com).

ABSTRACT: At first, the impact of selected spherically structured nanofillers made of different polar materials (carbon, silicon carbide, surface-modified silica, 2 wt % each) on mechanical properties of monomer cast polyamide 6 (MCPA6) was examined. Only the low-polar carbon-based nanofiller showed an average particle size below 100 nm in the liquid phase before polymerization was initiated. With regard to neat MCPA6, mechanical properties of the composite loaded with the carbon nanoparticles like tensile strength, Young's modulus, and heat distortion temperature could be improved by 6.4%, 13.5%, and 27.5%, respectively. The efficiency of carbon as filler material for MCPA6 was also shown for carbon short-cut fibers. A fiber content of 15% improved tensile strength from 78 to 93 MPa (19%) and Young's modulus could be doubled from 2660 MPa to nearly 5300 MPa. Regardless of the improved mechanical properties, the composites showed reduced degrees of crystallinity. Therefore, electron beam irradiation was applied to crosslink the polymer chains as an alternative to improve material properties. Crosslinking was supported by the application of a curing agent (CA). Two strategies for crosslinking experiments were tested: (1) Irradiation of CA-containing neat MCPA6 to find the most effective dose and subsequent treatment of the composites under this special condition; (2) Optimization of the properties by irradiation of the composites itself at graduated dose values. The second way was more convenient and showed, with regard to the composites without CA, improvements of tensile strength and Young's modulus of 6% each. © 2011 Wiley Periodicals, Inc. J Appl Polym Sci 123: 1201–1211, 2012

Key words: monomer cast polyamide 6; nanocomposites; carbon fibers; electron beam irradiation

INTRODUCTION

Due to high molecular weights and high degrees of crystallinity, monomer casting PA6 has several advantages over polycondenzation PA6.[1,2] With regard to the special polymerization reaction, anionic ring opening polymerization (AROP), different processing techniques like monomer casting,[3] rotational molding,[4] centrifugal molding,[5] and reaction injection molding[6] have been put to use. Following the trends in modern material development, nanofillers are in the focus of interest because of unexpected hybrid properties synergistically derived from the two components. Depending on the basic compositions of the nanofillers and their aspect ratios, improved mechanical and thermal properties,[7,8] gas permeability,[9] fire retardance,[10] or electrical conductivity[11] can be obtained compared with the pristine polymers.

Layered silicates, double layered hydroxides, and carbon nanotubes basically belong to the group of nanofillers with huge aspect ratios. The most commonly used layered silicate, clay, is montmorillonite (MMT).[12] To support exfoliation during nanocomposite preparation, MMT has been chemically modified by exchange of the small inorganic cations with voluminous organic cations. With respect to AROP of ε-caprolactam (CL), Liu et al. tested Na-MMT and an OMMT, modified with dioctadecyldimethylammonium cations.[13] Successful exfoliation was performed by the application of predispersants like water and acetone for Na-MMT and OMMT, respectively. They found that OMMT has a strong inhibiting effect on polymerization.[14] Traces of polar predispersants in the reaction system could partially deactivate the catalyst. A further approach to improve the application of pristine MMT as nanofiller for MCPA6 is the homoionical exchange of naturally occurring inorganic cations like sodium cations, for instance, by inorganic divalent cations like magnesium, calcium, or barium cations.[15] Special support for AROP is expected if the divalent cation of inorganically modified MMT is the same as that of the catalyst, like magnesium, for instance. The level of material properties mainly depends on prevention of sedimentation and the degree of exfoliation. The application of ammonium-terminated PMMA as compatibilizer for MCPA6/Na-MMT nanocomposites was studied by Wu et al.[16] The modifier

Correspondence to: G. Engelmann (Gunnar.Engelmann@iap.fraunhofer.de).

Contract grant sponsor: Federal Ministry of Economics and Technology and DECHEMA.

supports exfoliation and the exfoliated platelets limit the mobility of the polymer chains and, therefore, the degree of crystallinity.

As an example for continuous preparation of PA6/clay nanocomposites and as an alternative to melt compounding, Rothe et al.[17] published about reactive extrusion. CL was polymerized by AROP in the presence of an OMMT. First, the nanofiller was dispersed in the molten CL to support intercalation of the monomer into the galleries of the clays. After this, exfoliation of the platelets becomes supported by sheer stress. Other technical parameters like feeding time, for instance, are very important for a continuous flow of material.[18] Because working above the melting temperature of PA6 typical polymer properties of MCPA6 were abandoned. Compared with neat PA6 (extruded), elastic modulus of composites loaded with 4 wt % of OMMT was improved by 30–60%.

Carbon nanotubes (CNT), manufactured as single- or multiwall nanotubes, also belong to the group of nanofillers with huge aspect ratios. Besides the use of untreated CNT, their application focuses on pretreated CNT. In this case, pretreatment means mostly functionalization of the filler surfaces with hydroxyl-, carboxyl-, or carbonyl groups. Kelar et al.[19] reported about the application of nonpretreated MWCNT (0.05%, 0.1%, and 0.3%) in combination with a homogenizer. The composites were characterized by improved mechanical properties, strength and stiffness, increased thermal stability but lower degrees of crystallinity. Dongguang et al. gave examples for the successful application of hydroxyl functionalized MWCNT (0.05%, 0.1%, and 0.2%).[20] Dispersing in CL was supported by water as auxiliary dispersing agent. The polymer yields were in a range between 94 and 96% and the degrees of crystallinity were slightly improved (28.6–30.7%). In a second publication, Dongguang et al. described grafting of MCPA6 onto the surface of the carbon nanotubes.[21] For this purpose, MWCNTs were covalently functionalized with copoly(styrene-maleic anhydride).

The principle of grafting was also applied for spherically structured nanofillers like ε-caprolactam modified POSS (POSS-CL).[22] POSS-CL acts as physical crosslinking points and form nanometric crystalline aggregates. Structural characteristics of MCPA6 like branching, for instance, can be tailored by special polymerization conditions. Yang et al.[23] reported about the application of caprolactam-functionalized silica nanoparticles as an initiator for AROP. Toluene 2,4-diisocyanate (TDI) was used to bond CL to the particle surfaces. A monomer conversion off about 90% was achieved after 10 h and the molecular weight was in the order of magnitude of 10,000 g/mol.

Rusu et al.[24] applied a silica nanofiller both as received and modified with γ-aminopropyltrietoxysilane in combination with a special initiator (Sodium dicaprolactamato-bis(2-methoxyethoxo) aluminate) and activator (*N*,*N*′-[methylenedi(4,4′-phenylene)bis-carbamoyl]bis-ε-caprolactam) for the preparation of MCPA6 nanocomposites by rotational molding. The filler content was varied up to 10 wt %. With increasing filler content, reduction of the polymer yields, degree of polymerization, and degree of crystallinity was observed at a high level of material properties. Flexural strengths are characterized by a maximum at filler content of 4%. In contrast, flexural modulus shows a limiting value at 6%. There was an intensive gain in properties by the application of the modified silica nanoparticles.

High energy electrons can be used to modify polymers.[25–29] Polymer modification with high energy electrons is based on generation of excited atoms or molecules and ions for subsequent molecular changes via radical-induced chemical reactions. Depending on molecular structure of polymer as well as treatment conditions, it results in crosslinking, degradation (main-chain scission), grafting, curing, or polymerization. This kind of irradiation activates polymer chains by generating free radicals followed by recombination of different radicals to form stable sigma bonds. Generally, polymer chain degradation is an undesirable side reaction. In any case, optimization of technical parameters to support linking of intact polymer chains is the task to be solved for a given material. In preparation of this, curing agents (CA) should be applied. Such molecules are very flexible between the polymer chains and support bond formation. As the application of nanofillers and modified nanofillers, also in combination with auxiliary dispersing agents, curing agents can partially inhibit the AROP with consequences for molecular weight of the matrix polymer and the final properties of the composites.

In this study, the impact of commercially available spherical nanofillers made of carbon, silicon carbide, and hydrophobically modified silica on different material properties were tested without hydrophilic auxiliary agents. With regard to the success of carbon nanoparticles, carbon short-cut fibers were integrated into the experiments. Polyamide 6 belongs to those polymers preferring crosslinking after irradiation.[30] Therefore, electron beam irradiation was applied for additional improving of mechanical properties by crosslinking the polymer chains in the amorphous phase of the composites. Two different conditions of sample exposure were investigated:

1. Irradiation of CA-containing neat MCPA6 to find the most effective dose for treatment of the composites under this special condition.

2. Optimization of the properties by irradiation of the composites at graduated doses. The influence of dose, filler type, and filler content on the resulting properties was studied.

EXPERIMENTAL

Materials

ε-Caprolactam (CL) was purchased from Merck Schuchardt OHG (Hohenbrunn, Germany) and additionally purified by recrystallization. Both the catalyst Brüggolen® C 10 and the activator Brüggolen®C 20 P were ordered from Brüggemann Chemical KG (Heilbronn, Germany) for the polymerization reaction. Triallyl-s-triazin-2,4,6(1H,3H,5H)-trion (**1**) was purchased from Sigma-Aldrich (Seelze, Germany). Samples of Aerosil®R9200 (surface-modified silica) and Printex Alpha (carbon-based) were ordered from the former Degussa AG (Essen, Germany). Nanoparticles made of silicon carbide were purchased from Stanford materials Corp (Aliso Viejo, CA). Carbon short-cut fibers were ordered as sample from Toho Tenax Europe GmbH (Wuppertal, Germany).

Methods

Purification of ε-caprolactam

One hundred grams of ε-caprolactam were dissolved in boiling hexane. After hot filtration of the solution, precipitation starts. The white crystals were filtered out and carefully dried at 60°C in vacuum over wax.

Drying of the fillers

All nanofillers made of carbon and silicon carbide and the carbon short-cut fibers were dried at 200°C in vacuum for 8 h over phosphorus pentoxide. The surface-modified silica (Aerosol®R9200) was treated at 150°C for the same time.

Water content

The water contents were analyzed by Karl-Fischer (KF) method, performed with a Karl-Fischer-coulometer 756 in combination with a KF-oven (Metrohm AG, Herisau, Switzerland).

Polymerization

The preparation of polymers and compounds by the method of ε-caprolactam anionic polymerization was carried out in two separate glass reactors as follows:

- Reactor I was loaded with 2.8 g sodium lactamate and 47.2 g purified ε-caprolactam.
- Reactor II was filled with 2.1 g activator, X g filler, and (50-2.1-X) g CL ($X = 2$ g for nanofillers and accordingly 5, 10, or 15 g for carbon short-cur fibers).

The two glass reactors were tempered at 120°C in a nitrogen atmosphere. After complete melting, the fillers were dispersed by the application of ultrasound for 5 min. Subsequently, the content of reactor I was poured into reactor II by intensive stirring and further application of ultrasound for 1 min. Afterward, the tempered molding tool (160°C) was loaded immediately with the combined melt and annealed during 30 min at that temperature. At the end of the annealing period, the mold was cooled down to room temperature over night.

Pyrolysis

The samples were heated between 300 and 750°C in 50 K-steps for 30 min and at 750°C for 2 h.

DSC- and TGA

Measurements of the materials were performed with TA Instruments (New Castle, DE) DSC Q 1000 and TGA 500. The thermal behavior of the produced materials was examined in a temperature range of −50 to 350°C for DSC and −50 to 550°C for TGA. The rate for heating and cooling was 10 K/min. The DSC degree of crystallinity was calculated according to formula (1):

$$X_C = (\Delta H_m/(1-\phi)\Delta H_m^0) \times 100\% \quad (1)$$

- ΔH_m—the enthalpy of melting of a tested specimen, J/g,
- ΔH_m^0—the enthalpy of melting for a 100% crystalline standard of PA6 (230 J/g)[31]
- ϕ—the weight fraction of the filler in the composite.

Heat distortion temperature

Heat distortion temperature was measured in accordance to DIN EN ISO 75, practice A. However, a DMA (TA Instruments 2980) was used as the temperature chamber and the force applying device and therefore air instead of oil was used as surrounding medium. Comparison to proper ISO 75 measurements performed elsewhere showed that the DMA generated values are somewhat lower (in the order of 5 K) than the proper values.

Viscosimetry

The relative solution viscosity was determined by the viscosimeter device AVS 250 and the

temperature-controlling device CT 1450 of Schott Geräte GmbH (Ludwigshafen, Germany). Thus, 25, 50, 75, and 100 mg dry polyamide samples were weighed and dissolved under heating in concentrated sulfuric acid. The relative viscosity is determined at 25.0°C as a quotient η_{rel} of absolute viscosity (retention time) of the polymer solution η (t) and of the pure solvent η_0 (t_0) in an Ubbelohde viscometer; η_{spec} is defined by η_{rel}—1. The concentrations c of the polymer solutions of the composite samples were corrected with regard to the experimental amounts of filler components. Intrinsic viscosities were estimated according to the Huggins procedure based on linear correlations between η_{spec}/c and c.[32]

Particle counting

The nanoparticles size distribution from light diffraction were performed using a Coulter™ LS230 particle size analyzer (Beckman Coulter, Krefeld, Germany) with the polarization intensity (PIDS mode) included in the analysis. The samples were measured immediately after preparation. This particle analyzer can evaluate the particle sizes ranging from 0.0375 to 2000 μm. The size distribution was estimated by fitting the intensity of the scattered light ($\lambda = 750$ nm) as a function of the scattering angle ($\theta = 90°$).

Monomer content

The monomer contents of the neat polymers and composites were estimated by continuous extraction with boiling ethanol for 8 h. To support mass transfer from the bulk of the composites into the liquid phase, all samples were reduced to chip form and dried as described above to eliminate traces of humidity. The weights of the samples were analyzed before and after extraction and drying. From the resulting differences, the monomer contents were calculated as a quotient relative to the weight of the basic raw material.

Mechanical testing

Tensile strength and modulus of the composites were measured according to DIN EN ISO 527 and 178, respectively, with a universal testing machine (Zwick 020 (Ulm, Germany)) using the cast standard test specimen. However, the tensile modulus was determined as the maximum derivative at the beginning of the stress–strain curve measured at 50 mm/min testing speed.

Scanning electron microscopy (SEM)

A scanning electron microscope JSM 6330F (Jeol, Tokyo, Japan) was used at an acceleration voltage of 5 kV to study the morphology of sample cross sections. The cross sections were prepared by cryo-fracturing in liquid Nitrogen or with a rotating microtome (Leica RM 2255, Solms, Germany). Finally, the surfaces were sputtered with a Platinum-layer (thickness 4 nm) to avoid electrical charging by the electron beam.

Transmission electron microscopy (TEM)

The morphology of ultrathin cuts was studied with a transmission electron microscope CM 200 (Philips, Eindhooven, The Netherlands) at an acceleration voltage of 120 kV. The micrographs were taken with a digital camera MegaView II (Olympus, Hamburg, Germany). Ultrathin cuts (thickness $\sim$ 60 nm) were prepared with an UltraCut S (Leica, Germany). The samples were cut at −100°C with a diamond blade and finally deposited onto a foliated copper mesh (50 μm).

Irradiation

The samples were treated with accelerated electrons using an ELV-2 electron accelerator (Budker Institute of Nuclear Physics, Novosibirsk, Russia) installed in the Leibniz Institute of Polymer Research Dresden. The samples were placed on a pallet which was put on the conveyor system of irradiation facility and passed under the electron beam exit window with well-adjusted velocity to apply the desired dose to the samples. The samples were irradiated with doses of 5, 10, 20, 40, 80 to 160 kGy at about 25°C. The energy of the electrons and the beam current were 1.5 MeV and 4 mA, respectively. The irradiation facility is described in detail by Dorschner et al.[33]

RESULTS AND DISCUSSION

Selection of filler material

Deactivation of the sensitive MCPA6-catalyst ε-caprolactam sodium salt is possible by its intensive physical adsorption on the filler surfaces and especially by chemical reactions with their functional groups and humidity, attracted to the exposed solid surface. As a consequence, irreversible damaging reduces the effective concentration of the catalyst. It is expected that polar fillers increase the potential of danger. With regard to the reproducibility of the polymerization reaction and the material properties of the composites, negative influences should be minimized as far as possible. This is also a necessity to get high-molecular MCPA6. To test such graduation, three spherical nanofillers made of carbon (C), silicon carbide (SiC), and silica (SiO_2) were investigated. The filler content was kept constant at 2 wt % for all experiments with these particles. The polarity

TABLE I
Drying Temperatures, Drying Agents, and Water Contents of CL and the Different Fillers, All Samples Dried in Vacuum

Substance	$\Delta\chi$	H_2O-content (wt %)	T_{drying} (°C)	Drying agent
ε-caprolactam	–	0.03	60	Wax
Silica (Aerosil R 9200)	1.8	0.40	140	P_4O_{10}
Silicon carbide (SiC)	0.8	0.25	200	P_4O_{10}
Carbon (Printex Alpha)	0	0.15	200	P_4O_{10}
Carbon short-cut fiber	0	0.02	200	P_4O_{10}

graduation of the fillers can be roughly estimated by the difference of electronegativity values, $\Delta\chi$, according the periodic table of the elements they are made from. This means for C: $\Delta\chi_{CC} = 0$, for SiC: $\Delta\chi_{SiC} = 0.8$, and for SiO_2: $\Delta\chi_{SiO} = 1.8$. First experiments with a pure silica-based nanofiller showed in spite of careful drying problems in starting AROP. Therefore, silica nanoparticles with partially blocked OH-groups at the surface were applied (Aerosil R®9200). Chemically bonded aliphatic alkyl chains inhibited reactive centers, with consequences for the drying conditions. There was a limitation at nearly 140°C because of starting decomposition indicated by gently formation of smoke. The other thermally stable nanofillers were dried at 200°C (Table I).

The water content of the monomer could be reduced by recrystallization from 0.1% to 0.03%. With respect to the spherical nanoparticles, we detected a decrease of the water content from 0.4% to 0.15%, in correlation with the filler's polarity. The different water contents of the carbon-based fillers Printex Alpha and the short-cut fibers, 0.15% and 0.02%, respectively, can be interpreted as an indication for the highly adsorptive capacity of the nanofiller. Because of the remaining traces of humidity, the concentrations of activator and catalyst for AROP were fixed at 2.1% and 2.8%, respectively, for all experiments after some pre-examinations.

The degree of agglomeration of the different nanofillers is comparable and is somewhat independent on the basic materials. This means highly agglomerated spherical particles with average particle diameters in the range between 50 and 100 nm (Fig. 1).

The dry fillers were suspended in the monomer melt and dispersed by the support of ultrasound and stirring. Before polymerization, a sample was removed and diluted in an excess of ethanol. Such less corrosive dispersions could be analyzed by a sensitive particle counting device to register their particle size distribution curves (Fig. 2).

With regard to particle distribution in the monomer melt, this simplified procedure simulates particle agglomeration in a liquid phase with both polar (OH) and nonpolar (alkyl) characteristics. Obviously, the assumed polarities of the fillers influence the degree of agglomeration. Only the low-polar carbon particles show an intensive peak below 100 nm, followed by SiC-particles with a peak in the submicron range and the high-polar surface-modified SiO_2 ($\sim$ 10 μm).

The influence of the nanofillers on AROP is shown in the first instance by the monomer conversion and the intrinsic viscosities (IV) of the materials. Table II presents the data, IV-values were estimated according to the Huggins method.

All composites contained more soluble matter than neat MCPA6. The lowest degree of monomer conversion, 97.4%, was found for the composite loaded with silicon carbide. The comparatively low intrinsic viscosity (IV = 5.86 dL/g) correlates with this result. The carbon- or silica-based nanofillers seem to support MCPA6-formation better than silicon carbide. For both materials, monomer conversions of 98.3% each were estimated. The level of intrinsic viscosity is in the order of magnitude of the reference sample, with a benefit for modified silica. Taking the less successful experiments with pure silica as reference, we can see that surface modification of SiO_2 with aliphatic groups means a protecting effect for the polymerization reaction.

Additionally, Table II presents the crystallinity degrees X_C. It can be seen that the X_C-values of all composites are nearly identical (40–42%) and lower than that of neat MCPA6 (47%). Thostenson et al. suggest that the lower crystallinity seen in such composites is due to the inability of polymer chains to be fully incorporated into growing crystalline lamella.[34]

Tensile tests were performed to characterize the change of mechanical properties of the samples (Table III). The results indicate a weak increase of tensile strength from 78 MPa (neat MCPA6) to 83 MPa ($\sim$ 6%). In the case of spherical fillers, no significant improvements can be expected because of aspect ratios close to one. Stiffness becomes clearly enhanced from 2660 MPa up to 3020 MPa ($\sim$ 13%). The increase in Young's modulus correlates with a reduction of impact strength, except for the SiO_2 sample.

The graduation of Young's modulus correlates marginally with the average particle sizes of the spherical nanofillers dispersed in the liquid phase (Fig. 2). The better dispersed the fillers are the more rigid are the composites.

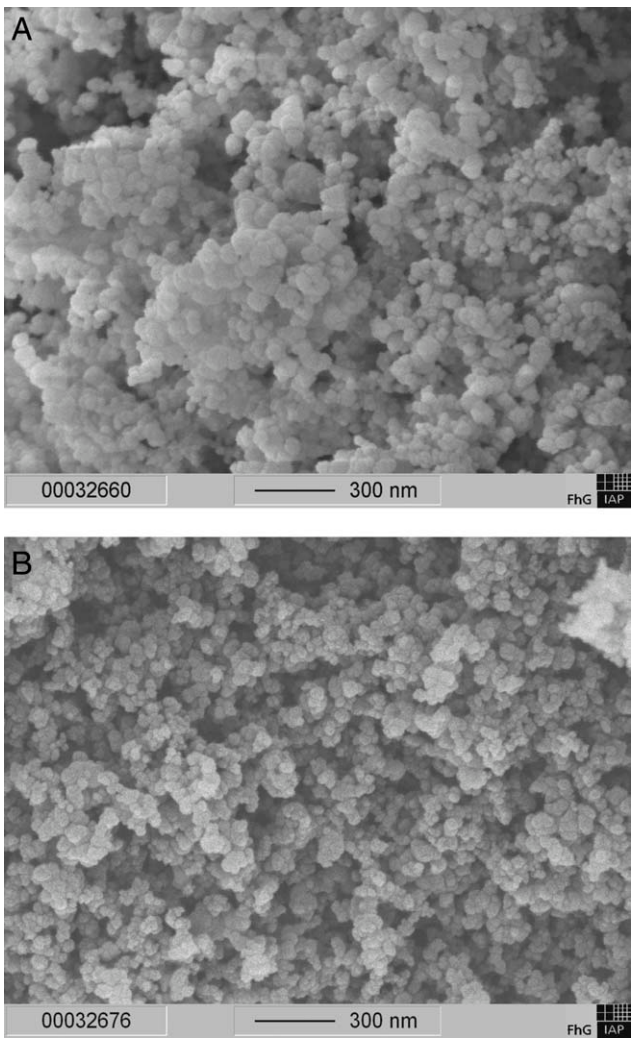

Figure 1 A: Agglomerated spherical fillers prepared from silicon carbide. B: Agglomerated spherical fillers prepared from carbon (Printex Alpha).

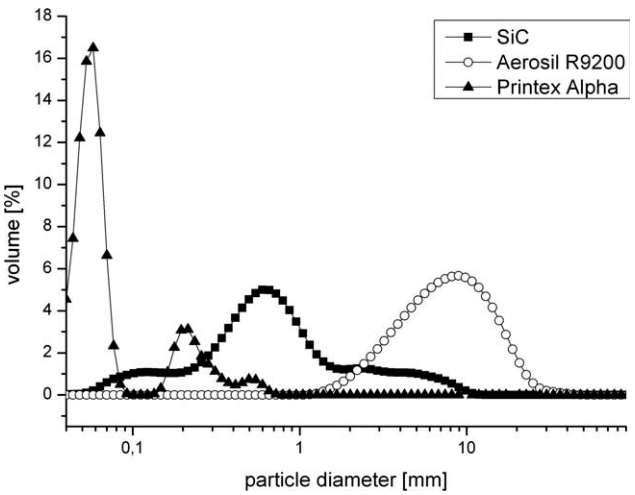

Figure 2 Particle size distribution of the nanofillers made of carbon (Printex Alpha), silicon carbide (SiC), and surface-modified silica (SiO_2), dispersed in ethanol by the support of ultrasound.

TABLE II
Intrinsic Viscosities According to Huggins (IV_H), Conversion, and Degrees of Crystallization of Neat MCPA6 and the Composites Loaded with C-, SiC-, and SiO_2-Based Nanofillers

Filler	Conversion (%)	IV_H (dL/g)	X_C (%)
–	99.0	6.77	47
SiO_2 (R9200)	98.3	7.76	40
C (Printex Alpha)	98.3	6.58	41
SiC	97.4	5.86	42

Heat distortion temperature (HDT) follows this trend, as well (Fig. 3).

With regard to the carbon filler, there is an enhancement of HDT by 28%.

According to the particle size distribution of the carbon filler in the liquid phase (Fig. 2), a TEM micrograph shows single carbon particles in the polymer matrix (Fig. 4).

Beside single particles, small aggregates were detected. This pattern differs marginally from expectation regarding the particle distribution in the liquid phase. A reason for this effect can be mixing of the two separately prepared monomer melts just before starting polymerization.

Taking all these facts into account, it becomes apparent that the less polar carbon nanofiller improve different mechanical properties by both protection of the AROP and their effective distribution in the polymer matrix. Because of the reduced crystallinity of this composite, electron beam irradiation was applied to try to improve material properties. Additionally, the influence of the filler itself on crosslinking efficiency can be investigated. In this context, another class of carbon-based reinforcing agents, important for cast technology, namely short-cut fibers (CF), is very interesting. In contrast to the spherical nanofillers, they belong to micro-scaled fillers with an aspect ratio >1 and complete an interesting set of fillers for these experiments. In this series of experiments, the maximum filler content and the resulting properties of the composites were in the focus of interest, as well. The morphology of the applied fibers is presented in Figure 5.

The fibers are characterized by rough surfaces. Because MCPA6 increase polymer density during

TABLE III
Results of Tensile Tests of Composites Loaded with Spherical Nanofillers, Dry Samples, Stored at 23°C

Filler	σ (MPa)	E (MPa)	a_{Cn} (kJ/m^2)
–	78 ± 3	2660 ± 30	6.8 ± 0.8
SiO_2 (R9200)	81 ± 1	2600 ± 130	3.5 ± 0.2
SiC	83 ± 1	2910 ± 40	4.8 ± 0.5
C (Printex Alpha)	83 ± 3	3020 ± 80	4.6 ± 0.3

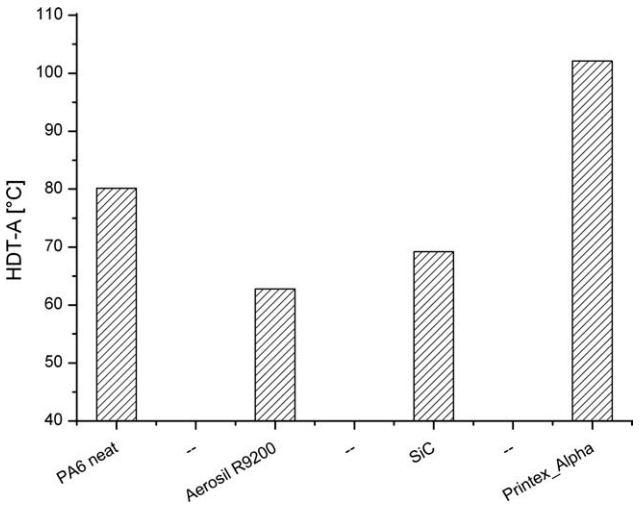

Figure 3 HDT-A of neat MCPA6 and composites loaded with spherically structured nanofillers.

cooling, an intensive contact between fiber and matrix by shrinking is possible.

The preparation of the composites was less problematic than in the case of the nanofillers. Samples with fiber contents up to 15% could be prepared. The mechanical results, tensile strength, and stiffness, correlate nearly linearly with the fiber content (Fig. 6).

Tensile strength was improved from 78 to 93 MPa (19%). Random distribution of these short-cut fibers in the polymer matrix prevents further improvements. The Young's modulus doubles from 2660 to 5300 MPa. Compared with the modulus of the nanocomposite (3020 MPa), this means an enhancement of 75%.

In all cases, the degree of crystallinity, X_C, of the composites, analyzed by DSC measurements, was lower than X_C of neat MCPA6 (Table IV).

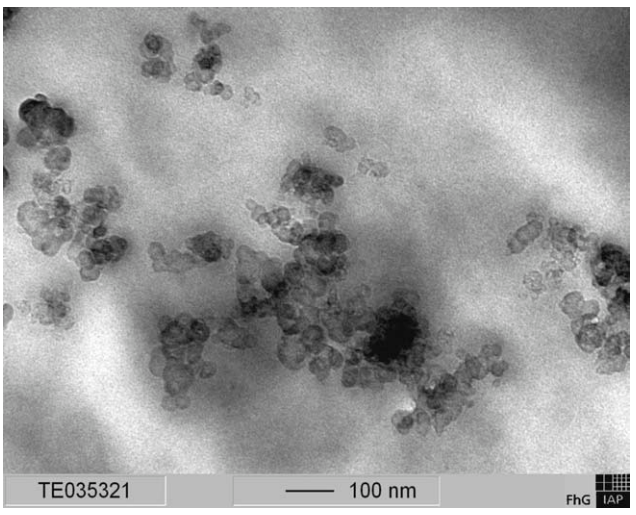

Figure 4 TEM-micrograph of dispersed carbon particles (Printex Alpha), distributed in the MCPA6-matrix.

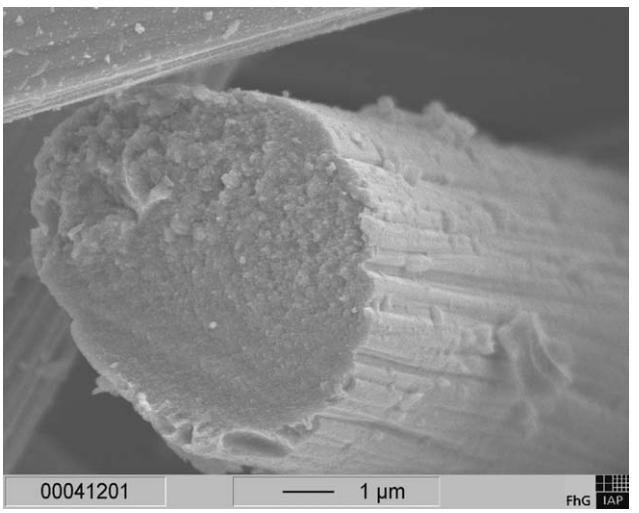

Figure 5 SEM-micrograph of carbon short-cut fibers.

X_C is between 40 and 42% and 33–40% for the nanocomposites and short-cut fibers, respectively. With respect to processibility and X_C, 10 wt % short-cut fibers were used for sample preparation to study irradiation effects.

Irradiation

Triallyl-s-triazin-2,4,6(1H,3H,5H)-trion (**1**) is suggested as CA for polyamides.[35] In general, with respect to the high susceptibility of AROP to foreign substances, the number of eligible chemicals is strongly limited. Substance **1** has no functional groups which could deactivate the catalyst sodium lactamate irreversibly and should be therefore convenient for these experiments.

To test the influence of this curing agent both on AROP and the material properties, MCPA6-samples with graduated contents of curing agent **1** (1–4%) were prepared and analyzed by stress–strain experiments (Fig. 7).

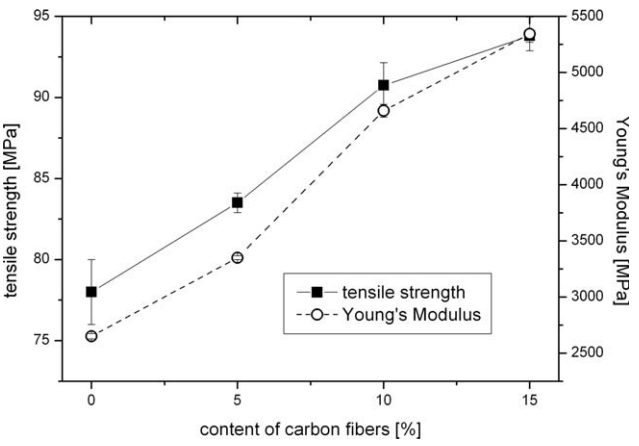

Figure 6 Influence of the carbon short-cut fiber content on selected mechanical properties.

TABLE IV
Degrees of Crystallinity, X_C, of MCPA6 and the Composites Loaded with the Different Types of Carbon-Based Fillers (Spherical Nanofiller, CF)

Filler	–	Printex Alpha	CF		
(wt %)	–	2	5	10	15
X_C (%)	47	40	33	36	40

Tensile strength decreases with increasing amount of curing agent **1** nearly linearly. In contrast, stiffness shows a positive impact at a content of 1%. Higher concentrations of substance **1** keep the moduli constant at nearly 2750 MPa. These data reveal that curing agent **1** acts as a softener. Based on this, samples containing 1 and 3% of curing agent **1** were prepared for detailed irradiation experiments.

The efficiency of irradiation on material properties can be studied by two strategies:

1. Application of graduated doses to CA containing MCPA6 samples and irradiation of the corresponding composites under this optimal condition
2. Optimizing the dose by irradiation of the composites at graduated doses

The second way includes interactions between matrix and filler during irradiation. Both methods were investigated.

First way

Dose values of 5, 10, 20, 40, 80, and 160 kGy were applied to MCPA6 containing 1 wt % or 3 wt % of curing agent **1**. Figure 8 shows the influence of irradiation on tensile strength and Young's modulus.

The MCPA6 samples containing 1 wt % CA show both for tensile strength and modulus a negligible dependency on the dose. All values are below the data of the untreated polymer. In contrast, the assays of MCPA6, containing 3 wt % of curing agent **1**, show real effects by irradiation at doses between 5 and 40 kGy. The gain compensates nearly the loss of properties by the presence of the curing agent. Therefore, only composites prepared with 3 wt % CA were in the focus of interest for further irradiation experiments. Filler contents of 2 wt % and 10 wt % for spherical nanoparticles and short-cut fibers, respectively, were examined. A dose of 20 kGy was fixed for these experiments. Figure 9 presents (for the carbon nanofiller, using tensile strength, and Young's modulus) the progress in material development step-by-step, beginning with neat MCPA6, followed by adding the curing agent (CA), loading with filler (F), both adding CA and loading the filler (CA+F), and finally irradiation.

The final impact of irradiation on mechanical properties is reflected best by comparing the irradiation data with those of neat MCPA6 and the

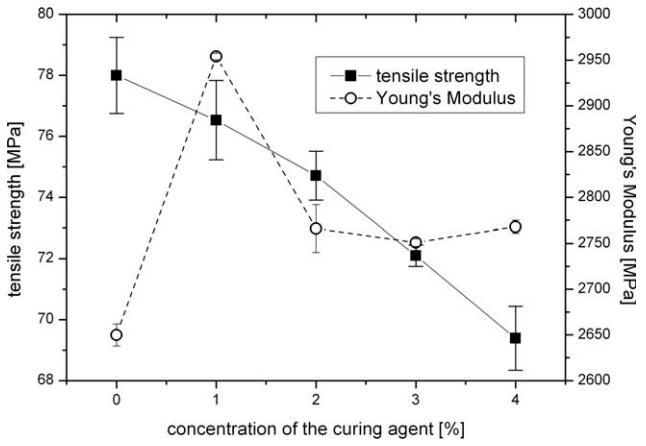

Figure 7 Dependence of tensile strength and Young's modulus on the concentration of curing agent **1**.

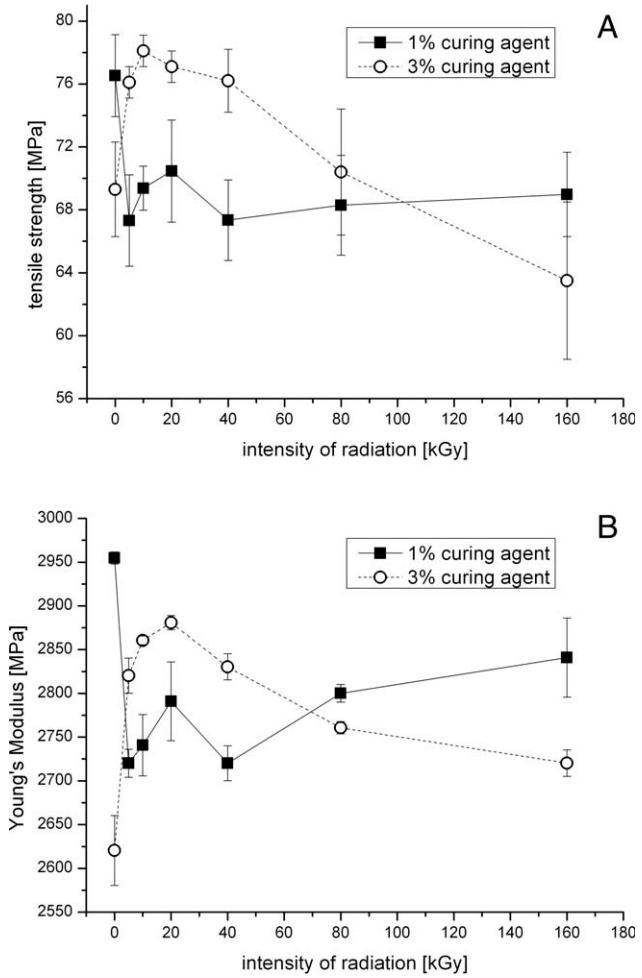

Figure 8 A: Tensile strength of MCPA6-samples prepared with 1 wt % or 3 wt % of CA **1**. B: Young's modulus of MCPA6-samples prepared with 1 wt % or 3 wt % of CA **1**.

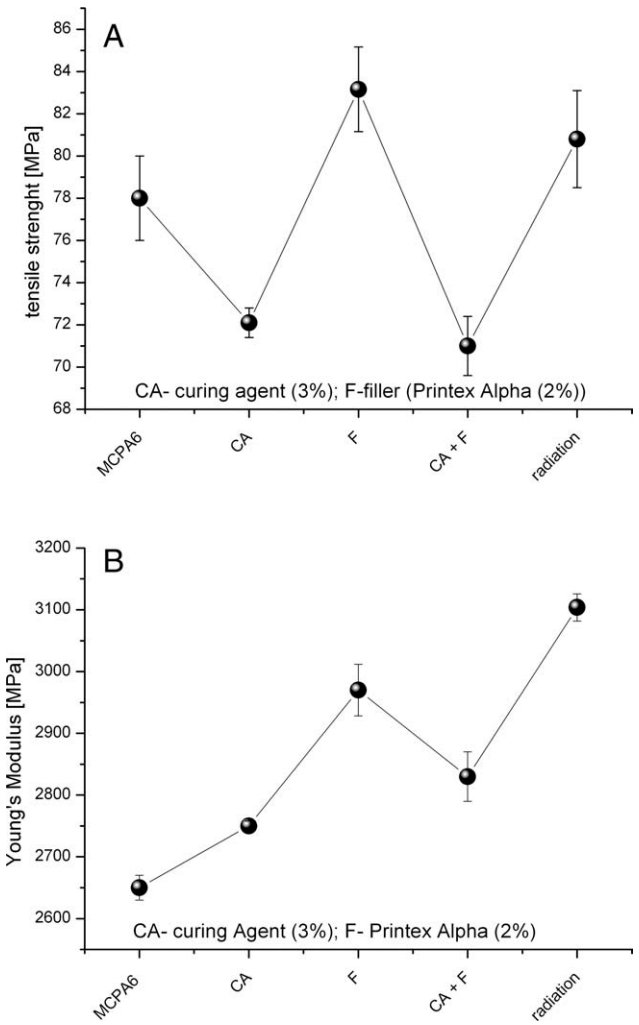

Figure 9 A: Tensile strength of neat MCPA6; MCPA6 + 3 wt % curing agent (CA); MCPA6 + 2 wt % spherical nanofiller (F); MCPA6 + 3 wt % CA + 2 wt % nanofiller (CA+F); MCPA6 + 3 wt % CA + 2 wt % nanofiller + 20 kGy (radiation). B: Young's modulus of neat MCPA6; MCPA6 + 3 wt % curing agent (CA); MCPA6 + 2 wt % spherical nanofiller (F); MCPA6 + 3 wt % CA + 2 wt % nanofiller (CA+F); MCPA6 + 3 wt % CA + 2 wt % nanofiller + 20 kGy (radiation).

composite not containing curing agent. The pure composites demonstrate, with regard to step-by-step material development, the peak values. In the case of tensile strength, we can see that the curing agent (3 wt %) overcompensates the gain of the nanofiller (2 wt %) (CA+F). Irradiation works but the σ-value does not exceed tensile strength of the composite (F). In contrast, stiffness has been really improved. Increases of 17 and 6% with regard to MCPA6 (neat) and CA+F, respectively, could be demonstrated.

The composites reinforced with 10 wt % carbon short-cut fibers are characterized by a higher impact on mechanical properties than the nanocomposites loaded with 2 wt % of spherical particles. Figure 10 shows that this gain in strength and stiffness (F) were only partially compensated by the curing agent (CA+F).

For the measured variables, tensile strength, and modulus, irradiation leads to marginal improvements of (CA+F), but the final values does not rise above the pure composite F.

Second way

The results of the first series of experiments were performed by irradiation of the composites with a constant dose which was optimized at CA-containing MCPA6. This method does not include effects like interactions between matrix and filler during exposure. To capture this, the composites loaded with 2 wt % spherical nanofiller or 10 wt % short-cut fibers and 3 wt % curing agent **1** each were

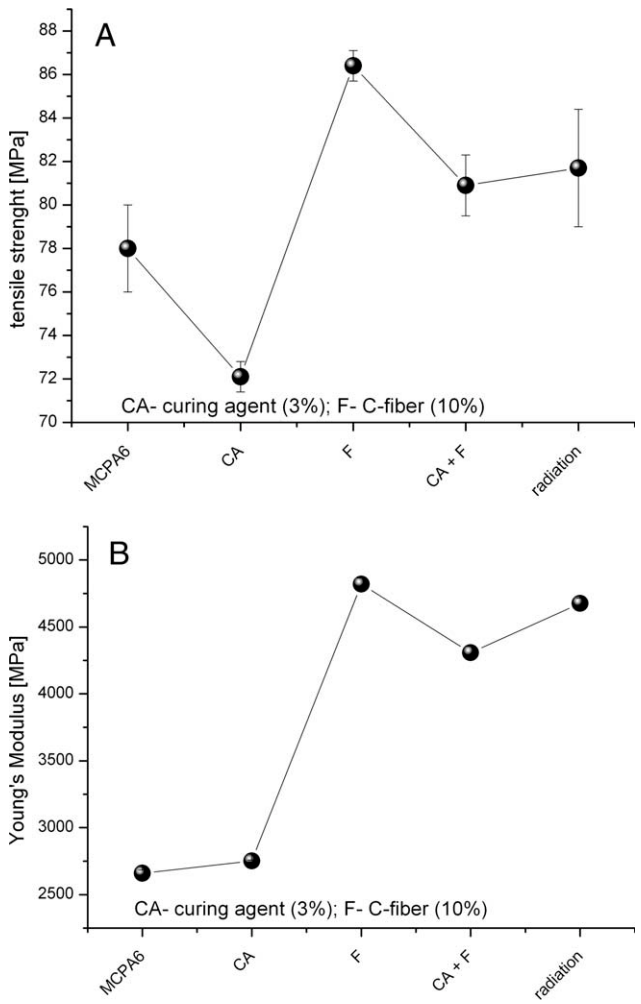

Figure 10 A: Tensile strength of neat MCPA6, MCPA6 + 3 wt % curing agent (CA), MCPA6 + 10 wt % filler (F), MCPA6 + 3 wt % CA + 10 wt % filler (CA+F), MCPA6 + 3 wt % CA + 10 wt % filler + 20 kGy (radiation). B: Young's modulus of neat MCPA6, MCPA6 + 3 wt % curing agent (CA), MCPA6 + 10 wt % filler (F), MCPA6 + 3 wt % CA + 10 wt % filler (CA+F), MCPA6 + 3 wt % CA + 10 wt % filler + 20 kGy (radiation).

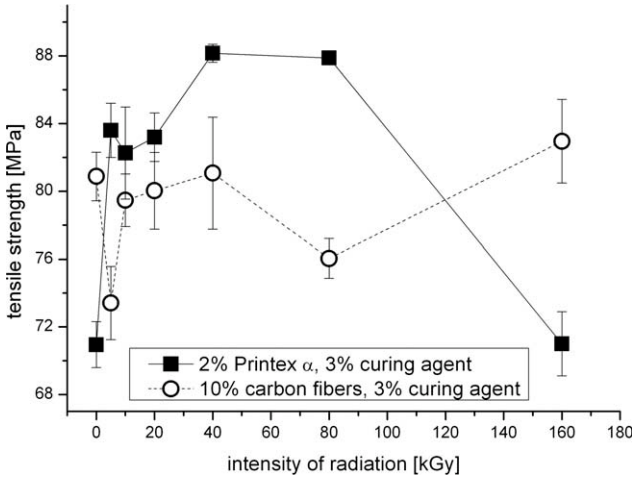

Figure 11 Change of tensile strength of composites loaded with 2 wt % Printex Alpha or 10 wt % carbon fibers and 3 wt % CA, by irradiation with graduated dose rates.

irradiated at the same graduated doses, as applied for the CA-containing MCPA6-samples (Fig. 8). In terms of Figure 9, describing the progress in material development step-by-step, Figure 11 presents results of the material combination (CA+F).

Improvements of tensile strength where achieved only for the nanocomposite. Compared with the results of the MCPA6/CA-samples, the optimal intensity of radiation was shifted from 20 kGy to 40–80 kGy. In this range, tensile strength was enhanced to 88 MPa. This means an increase of 6% in terms of the pure composite and an improvement of 13% with regard to neat MCPA6.

Young's modulus of the carbon fiber composite shows with nearly 4600 MPa a weak maximum at 5 kGy. This value is clearly below the modulus of the pure composite (5300 MPa). In contrast, stiffness of the nanocomposite is characterized by a maximum at 3200 MPa. The corresponding sample was treated with a dose rate of 40 kGy. The gain in Young's modulus is $\sim$ 6% (Fig. 12).

Irrespective of the two different irradiation procedures, we can see that only the nanocomposite, loaded with a minor filler content of 2 wt %, shows positive effects. The high impact of the short-cut fibers (10 wt %) on the material properties could not be exceeded.

CONCLUSIONS

Tests with selected spherical nanofillers made of different materials like carbon, silicon carbide, and surface-modified silica show that mechanical properties of their MCPA6-composites could be improved best by the less polar carbon-based nanofiller. This is possible because of protection of the sensitive anionic ring opening polymerization reaction and the well-distributed nanoparticles both in the liquid phase before polymerization and, finally, in the composites. Especially strength, stiffness, and heat distortion temperature of the composites have been improved by 6.4%, 13.5%, and 29%, respectively, at a filler content of 2 wt % each.

The efficiency of carbon for applications in the field of MCPA6 can be expanded to short-cut fibers as well. Their processibility is limited by the viscosity of the fiber containing monomer melt. This means a maximum content of 15 wt % for short-cut fibers. While tensile strength of the fiber composite (15 wt %) was enhanced from 78 to 93 MPa, stiffness has been doubled from 2660 to 5300 MPa.

With regard to neat MCPA6, the degrees of crystallinity of the carbon composites were generally reduced, as far as 16% at a fiber content of 15 wt %. Electron beam irradiation has been applied with varying success to improve the composite's properties by crosslinking the polymer chains in the amorphous phase of the materials. To support curing and with respect to the very sensitive anionic ring opening polymerization, the curing agent (CA) Triallyl-s-triazin-2,4,6(1H,3H,5H)-trion was finally applied in a concentration of 3 wt %. Composites loaded with 2 wt % spherical nanofillers or with 10 wt % short-cut fibers were studied in more detail. Two crosslinking experiments were separately tested: (1) Irradiation of CA-containing neat MCPA6 to find the most effective dose for treatment of the composites under this special condition; (2) Optimization of the properties by irradiation of the composites at graduated doses. The second way was more successful. The presence of the fillers shifts doses from 20 kGy, identified during the first series of experiment, to 40–80 kGy. Only the composites loaded with 2 wt % spherical

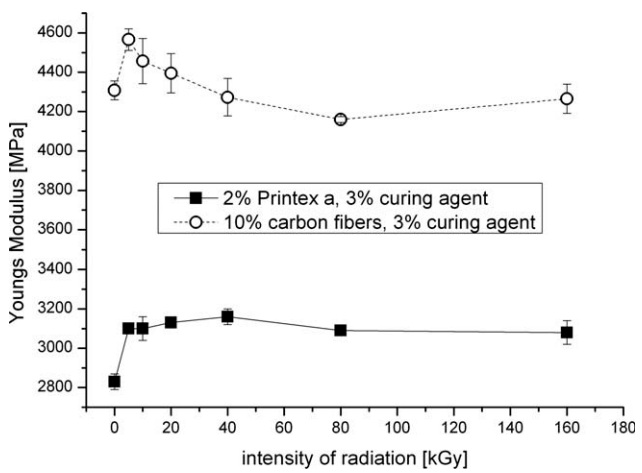

Figure 12 Change of Young's modulus of CA-containing composites loaded with 2 wt % Printex Alpha or 10 wt % carbon short-cut fibers by irradiation with variable dose rates.

carbon nanofiller show a gain in mechanical properties. Both tensile strength and Young's modulus were improved by 6% each. In contrast, the presence of the short-cut fibers (10 wt %) seems to predominate the impact of irradiation.

References

1. Hall, H. K., Jr. J Am Chem Soc 1958, 80, 6404.
2. Rusu, G.; Ueda, K.; Rusu, E.; Rusu, M. Polymer 2001, 42, 5669.
3. Kircher, K. Chemical Reaction Plastics Processing; Hanser Publishers: Munich, 1989; p 78.
4. Rusu, G.; Rusu, E. High Perform Polym 2004, 16, 569.
5. Rusu, G.; Rusu, M.; Rusu, E.; Stoleriu, A.; Teaca, C.-A. Polym Plast Technol Eng 2000, 39, 233.
6. Macosko, C. W. RIM Fundamentals of Reaction Injection Molding; Hanser Publishers: Munich, 1989; p 182.
7. Kelnar, I.; Kotek, J.; Kapra'lkova', L.; Munteanu, B. S. J Appl Polym Sci 2005, 96, 288.
8. Pramoda, K. P.; Liua, T.; Liua, Z.; Hea, Ch.; Sue, H.-J. Polym Degrad Stab 2003, 81, 47.
9. Merkel, T. C.; He, Z.; Pinnau, I.; Freeman, B. D.; Meakin, P.; Hill, A. J. Macromolecules 2003, 36, 6844.
10. Laoutid, F.; Ferry, L.; Leroy, E.; Cuesta, J. M. L. Polym Degrad Stab 2006, 91, 2140.
11. Valentino, O.; Sarno, M.; Rainone, N. G.; Nobile, M. R.; Ciambelli, P.; Neitzert, H. C.; Simon, G. P. Phys E 2008, 40, 2440.
12. Suprakas Sinha, R.; Okamoto, M. Prog Polym Sci 2003, 28, 1539.
13. Liu, A.; Xie, T.; Yang, G. Macromol Chem Phys 2006, 207, 1174.
14. Liu, A.; Xie, T.; Yang, G. Macromol Chem Phys 2006, 207, 701.
15. Kadlecová, Z.; Puffr, R.; Baldrian, J.; Schmidt, P.; Roda, J.; Brožek, J. Eur Polym J 2008, 44, 2798.
16. Wu, T.; Liu, A.; Yang, T. G. J Polym Sci Part B: Polym Phys 2008, 46, 1802.
17. Rothe, B.; Elas, A.; Michaeli, W. Macromol Mater Eng 2009, 294, 54.
18. Park, J. H.; Kim, W. N.; Kye, H.-S.; Lee, S.-S.; Park, M.; Kim, J.; Lim, S. Macromol Res 2005, 13, 367.
19. Kelar, K.; Jurkowski, B. J Appl Polym Sci 2007, 104, 3010.
20. Yan, D.; Xie, T.; Yang, G. J Appl Polym Sci 2009, 111, 1278.
21. Yan, D.; Yang, G. Mater Lett 2009, 63, 298.
22. Ricco, L.; Russo, S.; Monticelli, O.; Bordo, A.; Bellocci, F. Polymer 2005, 46, 6810.
23. Yang, M.; Gao, Y.; He, J. P.; Li, H. M. Express Polym Lett 2007, 1, 433.
24. Rusu, G.; Rusu, E. High Perform Polym 2006, 18, 355.
25. Thakur, V.; Leuteritz, A.; Gohs, U.; Kretzschmar, B.; Wagenknecht, U.; Bhowmick, A. K.; Heinrich, G. Appl Clay Sci 2010, 49, 200.
26. Khan, M. S.; Franke, R.; Gohs, U.; Lehmann, D.; Heinrich, G. Wear 2009, 266, 175.
27. Vasiljeva, I. V.; Mjakin, S. V.; Makarov, A. V.; Krasovsky, A. N.; Varlamov, A. V. Appl Surf Sci 2006, 252, 8768.
28. Liu, H.; Fang, Z.; Peng, M.; Shen, L.; Wang, Y. Radiat Phys Chem 2009, 78, 922.
29. Sengupta, R.; Tikku, V. K.; Somani, A. K.; Chaki, T. K.; Bhowmick, A. K. Radiat Phys Chem 2005, 72, 751.
30. Lyons, B. J.; Glover, L. C. Radiat Phys Chem 1991, 37, 93.
31. Khanna, Y. P.; Kuhn, W. P. J Polym Sci Part B: Polym Phys 1997, 35, 2219.
32. Elias, H.-G. Makromoleküle Band 2; Wiley-VCH: Weinheim/New York/Chichester/Brisbane/Singapore/Toronto, 2001; p 400.
33. Dorschner, H.; Lappan, U.; Lunkwitz, K. Nucl Instrum Methods B 1998, 139, 495.
34. Thostenson, E. T.; Ren, Z.; Chou, T. W. Compos Sci Technol 2001, 61, 1899.
35. Ueno, K. Radiat Phys Chem 1990, 35, 126.